Golden Rule Study of Excited-State Proton Transfer in 2-(2′- Hydroxyphenyl)benzoxazole and 2-(2′-Hydroxy-4′-methylphenyl) benzoxazole

ARTICLE *in* THE JOURNAL OF PHYSICAL CHEMISTRY · JANUARY 1993

Impact Factor: 2.78 · DOI: 10.1021/j100104a009

3 AUTHORS, INCLUDING:

Venelin Enchev
Bulgarian Academy of Sciences
103 PUBLICATIONS **784** CITATIONS

SEE PROFILE

Golden Rule Study of Excited-State Proton Transfer in 2-(2'-Hydroxyphenyl)benzoxazole and 2-(2'-Hydroxy-4'-methylphenyl)benzoxazole

L. Lavtchieva, V. Enchev, and Z. Smedarchina*

Institute of Organic Chemistry, Bulgarian Academy of Sciences, 1113 Sofia, Bulgaria

Received: August 25, 1992; In Final Form: October 20, 1992

Theoretical Golden Rule treatment of the dynamics of triplet and singlet excited-state intramolecular proton transfer (ESIPT) in 2-(2'-hydroxyphenyl)benzoxazole (HBO) and its derivative 2-(2'-hydroxy-4'-methylphenyl)-benzoxazole (MHBO) is presented. These compounds express typical and very similar non-Arrhenius temperature behavior of the rate of triplet keto–enol equilibration $\theta_l = k_{K-E} + k_{E-K}$ despite the experimental evidence of different reaction regimes and keto–enol energy gaps. In the method applied, all modes of the transferred atom (stretching, bending, and twisting) are taken into account, including an effective intramolecular promoting mode coupled to the H-motion, which is mainly responsible for the temperature dependence of the rate constant. Input data for the dynamic calculations is the standard output of the AM1 (structural and force field) results for both tautomers; the electronic coupling integral J is an adjustable parameter. The calculated rate θ_l is only slightly sensitive to the two experimentally suggested arrangements of the enol and keto triplet states ($\Delta E = E_K - E_E = 0$ and 9.9 kJ/mol for HBO and MHBO, respectively), as experimentally observed, and is in good agreement with the experimental results for both isotopes. The study of the singlet ESIPT in these compounds suggests that the primary reason for the rapidity of the process, as well as for the distinctions between the triplet and singlet transfer, is in electronic factors, mainly the electronic coupling.

I. Introduction

The excited-state proton-transfer reactions in intramolecularly H-bonded species (ESIPT) are the most widely investigated proton-transfer (PT) reactions and are subject of an enormous number of studies.[1-11] Their common feature is their unusual rapidity even at low temperatures: the rate constants for singlet ESIPT as a rule exceeds 10^{11} s^{-1},[1] thus being several orders of magnitude faster than any of the reported ground-state H-transfer reactions. Unfortunately, experimental constraints prevent so far the obtaining of definite evidence which could allow an unambiguous assignment of the ESIPT mechanism. On the other hand, the excited states of the large molecules undergoing ESIPT are hardly accessible for quantum-chemical studies of their potential energy surfaces (PES) accurate enough to serve the goals of the theoretical description of the reaction dynamics. On the basis of the available experimental data and qualitative considerations, three types of PT mechanisms are discussed at present[1,2] which require specific theoretical treatment: (i) barrierless transition on a single-minimum PES;[1-3] (ii) tunneling through a low barrier of height commensurate with the zero H-vibrational level;[1,2] (iii) "deep" tunneling through a considerably higher barrier.[2]

Among the few examples of ESIPT systems with well-studied kinetics of both H- and D-transfer[4-11] which permit unambiguous assignment of the transfer mechanism as a tunneling process of type iii is 2-(2'-hydroxyphenyl)benzoxazole (HBO) and its slightly modified derivative 2-(2'-hydroxy-4'-methylphenyl)benzoxazole (MHBO). Being the only systems for which the temperature dependence of the rate constant has been traced down to the low-temperature limit for both isotopomers, HBO and MHBO present a unique opportunity for testing theoretical models. In the present paper, the ESIPT dynamics in HBO and MHBO is studied by the Golden Rule (GR) method combined with semiempirical AM1 calculations which produce the input data for the dynamic analysis. The GR approach is especially well suited for processes where many modes are expected to contribute; it has proven its efficiency for ground-state H-tunneling reactions[12-17] and intermolecular solid-state ESPT.[18] For the system at hand, such a combined study would be particularly revealing with respect to the limitations and capabilities of this way of approaching the ESIPT dynamics in real systems of interest, which are mainly large organic molecules, because so far the semiempirical methods seem to be the only tool of theoretical investigation.

The paper is organized as follows. Section II reports on the features of the triplet and singlet reaction dynamics; section III represents the theoretical methods applied: AM1 for structural and force-field calculations, and Golden Rule for dynamics calculations; in section IV we discuss the results for triplet and singlet ESIPT and end with the main conclusions.

II. The Reaction Dynamics

In HBO and MHBO (Figure 1) both singlet and triplet ESIPT were reported. The whole photophysical scheme of the processes following the excitation of HBO (and MHBO) is presented in Figure 2 according to refs 5–10. The ultrafast singlet PT with a rate constant of H-transfer $k_H \geq 3 \times 10^{12}$ s^{-1} [6] prevents the deactivation of the excited enol form through any other channel, and the triplet keto form is populated exclusively via intersystem crossing from the singlet keto tautomer. The triplet ESIPT, which is significantly slower than the singlet ESIPT ($k_H \simeq 10^{7.4}$ s^{-1} at 200 K), was extensively studied and shows typical H-tunneling kinetics with non-Arrhenius temperature behavior of the rate constant. No data was reported on the reverse ground-state PT. The experimental evidence suggests that the triplet ESIPT in HBO proceeds between isoenergetic keto and enol forms and an equilibrium is established within the triplet-state lifetime, while in the MHBO triplet ESIPT is virtually unidirectional from the keto to the enol tautomer with a keto–enol gap of at least 330 cm^{-1}.[9,10] This conclusion is based on the following main observations: (i) dual phosphorescence in HBO with temperature-independent intensity ratio in fluid solutions; in MHBO keto phosphorescence cannot be observed; (ii) monoexponential triplet decay of HBO in liquid solutions and polyexponential decay in solid solutions; the MHBO triplet decay is always monoexponential; (iii) the values of the rate constants obtained from the transient-absorption experiments are in good agreement with those obtained from the phosphorescent measurements. Both H- and D-transfer rate constants of the bidirectional triplet ESIPT in HBO and the unidirectional one in MHBO are very close in

0022-3654/58/2097-0306$04.00/0

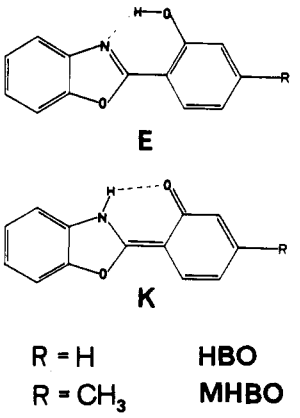

Figure 1. The ESIPT reaction in HBO and MHBO.

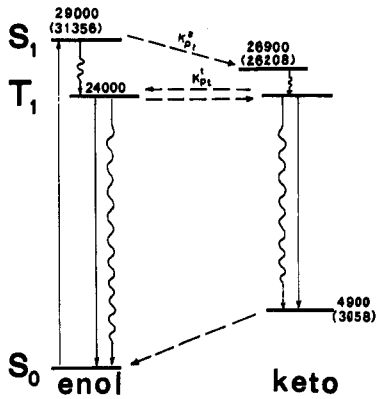

Figure 2. Diagram of the levels involved in the photophysical cycle of HBO.[5-10] The energies are in cm^{-1}; the AM1 values are given in parentheses.

value: the ratio $k_{K\text{-}E}^{HBO}/k_{K\text{-}E}^{MHBO}$ is temperature independent and equal to ca. 1.3.[9,10]

III. AM1 and GR Calculations

We start this section with the results of semiempirical (AM1) analysis of the triplet and singlet states involved in the ESIPT, which will be implemented into the dynamics calculations of section III.B.

A. Semiempirical Quantum-Chemical Analysis. The calculations were performed with the MOPAC 6.0 program package.[19] The AM1 method[20] was chosen since it takes hydrogen bonds into account. The geometry optimization was carried out with the eigenvector following (EF) routine;[21] the PRECISE keyword was employed in all cases except for the S_1 state. In the S_1 calculations the OPEN(2,2) keyword was used. The triplet-state calculations were carried out with the unrestricted Hartree–Fock formalism using keywords UHF and TRIPLET. Force-field calculations were also performed using the optimized geometries of the tautomers in S_0, S_1, and T_1 states.

AM1 calculations render, rather surprisingly, a nonplanar keto triplet tautomer with both the *o*-hydroxyphenyl moiety and the H-atom of the NH bond situated out of the plane of the benzoxazole skeleton of the molecule. In addition, the *o*-hydroxyphenyl fragment is twisted around the C–C′ bond at an angle of 57°. A planar keto form was found under constrained optimization (with all dihedrals fixed to planarity), but all attempts to search for it by full optimization failed. The calculations produced no substantial difference between the triplet tautomers of HBO and MHBO, either in geometries or in their relative energies. The enol–keto energy gap $\Delta E = E(\text{enol}) - E(\text{keto})$ is ca. 9.9 kJ/mol for the nonplanar keto form (for both HBO and MHBO) and 1.9 kJ/mol for the planar keto structure, found for HBO. However small, these gaps are of opposite signs to those resulting from experiments; we discuss this in more detail below.

TABLE I: AM1 Structural and Spectroscopic Parameters for the S_1, S_0, and T_1 States of HBO[a]

	R_{NO}, Å	ω_{str}^{H}, cm^{-1}	ω_{bend}^{H}, cm^{-1}	$r_{N(O)H}$, Å	ΔE, kJ/mol	l, Å
			S_1			
e	2.89	3332	1396	0.97		
k	2.72	3372	1378	0.99	63.8	1.34
			T_1			
e	2.98	3422	1407	0.97		
npl	2.86	3386	1360 690	0.99	9.9	1.64
pl	2.80				1.2	1.46
			S_0			
e	2.97	3391	1505	0.97		
k	2.76	3397	1386	0.99	37.9	1.43

[a] Here, pl and npl denote the planar and nonplanar keto triplet form; l is the tunneling distance; $r_{N(O)H}$ is the NH (respectively OH) equilibrium bond length. Two bending H-vibrations relevant to the transfer are reported for the nonplanar triplet keto tautomer.

Some geometric parameters, the characteristic H-frequencies, and ΔE for S_1, T_1, and S_0 states of HBO, as calculated by AM1, are listed in Table I.

B. Dynamics Calculations. To treat the proton-transfer dynamics, a version of the Golden Rule (GR) approach was employed, generalized for large values of the electronic coupling.[13-15] Here we report briefly on the specific features of the GR version applied.

According to the Golden Rule of time-dependent perturbation theory the rate constant of hydrogen transfer between two heavy atoms D and A (donor and acceptor) in the complex D···H···A can be presented in the form

$$k_{GR} = \frac{2\pi}{\hbar} \mathrm{Av} \sum |\langle \prod_j \Psi_j^{f} | J | \prod_j \Psi_j^{i} \rangle|^2 \rho(E_i - E_f) \qquad (1)$$

Here the irreversibility of the transition is secured by the high density ρ of energy conserving final states due to the coupling to the low-frequency modes including those of the solvent. In the matrix element between the initial and final state (i and f, respectively), J is the electronic coupling integral, and the vibrational wave functions Ψ_j include both the high-frequency H-modes and the low-frequency intramolecular D···A vibrations coupled to the H-modes. These low-frequency modes are mainly responsible for the temperature dependence of the rate constant, their effect on the tunneling distance and barrier height known as barrier fluctuation effect (see, e.g. ref 16 and the literature therein). Thus we divide the low-frequency vibrations into two groups: (i) intramolecular soft modes coupled to the H-motion, thus promoting the transfer, and (ii) solvent modes mainly responsible for relaxation effects, thus securing the irreversibility of the transfer. The sum in eq 1 runs over all vibrational quantum numbers in the final state, Av denotes equilibrium average in the initial state. According to the scheme proposed earlier[13-15] eq 1 can be generalized to the case of arbitrary coupling; then the rate constant of the transfer is a product of k_{GR} and a correction for adiabaticity $\Lambda(J)$ which depends only on the electronic coupling and the parameters describing the H-motion. In the two-dimensional (2D-GR) version of the GR model[12] two vibrational modes are taken: one H-mode with effective frequency calculated on the basis of the characteristic H-vibrations, and one low-frequency mode responsible for the barrier modulation. Here, the effective H-mode is described as a Morse oscillator with frequency

$$\omega_{eff} = (\sum_k \omega^2{}_k \cos^2 \theta_k)^{1/2} \qquad (2)$$

ω_k being the relevant H-vibrations—stretching, bending, and twisting—θ_k the angles between the H-atom displacement in the ith vibration and the vector connecting the initial and final

H-positions; the anharmonicity parameter x is taken to be equal to that of the stretching mode.

Normally it is not just one "skeletal" mode which is coupled to the H-motion and thus significantly affects the geometry of the reaction complex.[12,16,17,22] Therefore a question arises as to whether it is possible to construct an effective skeletal oscillator whose parameters (effective frequency and mass) comprise all of the information about the set of participating intramolecular modes and has the same effect on the rate constant. This problem was discussed for intramolecular H-transfer and for intermolecular reactions in solids.[17,22] In both cases it was possible to introduce such an effective low-frequency oscillator since the "skeletal" vibrations affect the tunneling distance (and thus the rate constant) only modulating it by an effective amplitude $A_{\text{eff}}^2 = \sum_k \alpha_k^2 \coth \hbar\Omega_k/2k_BT$[22] where the coefficients α_k define the contribution of the normal vibrations $\{q_k\}$ with frequencies $\{\Omega_k\}$ to the donor–acceptor displacement. By the equation

$$A_{\text{eff}}^2 = \frac{\hbar}{\Omega_{\text{eff}}\mu_{\text{eff}}} \coth \hbar\Omega_{\text{eff}}/2k_BT \qquad (3.1)$$

we define the effective mode; its parameters Ω_{eff} and μ_{eff} can be found from the low- and high-frequency limits of eq 3.1 as

$$\Omega_{\text{eff}} = A_0^2/\sum_k(\alpha_k^2/\Omega_k) \qquad \mu_{\text{eff}} = \hbar\sum_k(\alpha_k^2/\Omega_k)/A_0^4 \qquad (3.2)$$

if the temperature interval of interest is not very large (which is normally well met in the kinetic experiments); $A_0^2 = \sum_k \alpha_k^2$. All sums run over those normal vibrations which are not ruled out by symmetry restrictions.

The relative displacement of the atoms carrying the proton can be expressed via the $3N(3N-6)$ matrix L which describes the mass-weighted atomic displacements in terms of normal coordinates; then, for the model of the "linearized" reaction complex adopted here, the coefficients α_k are given by the following expression

$$\alpha_k = (\hbar/\mu\Omega_k)^{1/2}\Delta L_k$$

where $\Delta L_k = [\Delta L_{kx}^2 + \Delta L_{ky}^2 + \Delta L_{kz}^2]^{1/2}$, and $\Delta L_{kn} = L_{kn}^{\text{D}} - L_{kn}^{\text{A}}$, $L_{kn}^{\text{D(A)}}$ (n = x, y, z) being the matrix element for the donor (acceptor) atom, and μ being their reduced mass. The matrix L, the normal modes' symmetry, and their frequencies are supposed to be available from force-field calculations for the reaction complex.

With this done, the evaluation of the Golden Rule rate constant k_{GR} in eq 1 can follow simple numerical procedure with just two degrees of freedom (for the 2D-GR version): one effective high-frequency oscillator and one effective low-frequency oscillator with parameters defined by eqs 2 and 3.2, respectively. The density of final states in eq 1 is represented by a Gaussian function whose half-width is taken for simplicity to be equal to $\hbar\Omega_{\text{eff}}/2$. The correction parameter $\Lambda(J)$ accounting for the coupling strength has the form[15]

$$\Lambda(J) = \hbar\omega_{\text{eff}}(E_r - \Delta E)\exp(b_{\text{eff}}J)/J^2$$

$$b_{\text{eff}} = \{(2^{1/2}-1)(4\pi J/\hbar\omega_{\text{eff}})(1-(\hbar\omega_{\text{eff}}/8U_0^{\text{d}})^{1/2})\} \qquad (4)$$

with U_0^{d} being the height of the diabatic barrier, i.e., the crossing point of the potentials describing the initial and final products, E_r the (reorganization) energy (necessary to move along the coordinate of the transferred particle from the initial to the final equilibrium position in the initial electronic state), ΔE the exothermicity of the reaction, and J the only adjustable parameter. Finally the rate constant of transfer is given by the product

$$k = k_{\text{GR}}\Lambda(J) \qquad (5)$$

This concludes the description of the two-dimensional (2D-GR) version applied in the present paper; the three-dimensional implementation (3D-GR) includes the H-bending and stretching modes explicitly in the transition matrix element in eq 1 besides the soft mode, and is directly applicable to nonlinear planar systems. For both versions, all necessary parameters leading to the rate constant (eq 5) can be constructed using the standard output of the AM1 calculations.

IV. Results and Discussion

In this section we apply the GR version reported above to the kinetics of triplet and singlet ESIPT in HBO and MHBO. On the example of this system, we concentrate mainly on the methodological analysis of the limitations and reliability of these methods to PT in the excited states of polyatomic molecules.

Judging by the kinetics of the triplet ESIPT in HBO and MHBO, it obviously belongs to the "deep-tunneling" processes, to which GR treatment can be straightforwardly applied. We discuss here two possible mechanisms of the reaction: H-transfer between planar enol and keto tautomers (planar mechanism), and H-transfer between a nonplanar keto form and a planar enol form (nonplanar mechanism). The first seems to be more likely than the second (suggested by the AM1 results) because of the following reasons: (i) the tunneling distance (l = 1.46 Å) of the "planar" ESIPT is significantly shorter than that of the "nonplanar" ESIPT (l = 1.64 Å); (ii) the ESIPT rate does not depend on the solvent viscosity; this observation seeming to be in contrast to the considerable "skeleton reorganization" accompanying the "nonplanar" ESIPT; (iii) the nonplanar keto form was found to be less stable than the enol tautomer by ca. 2.2 kcal/mol, while the planar forms were calculated to be nearly isoenergetic (ΔE = 0.45 kcal/mol) which is more consistent with the experiment (section II). Of course, this latter argument is not decisive, as AM1 is not well tested for excited states, and thus, the reliability of its results is unknown a priori. However, since a planar keto triplet form was not found in full (i.e., inclining the dihedrals) optimization and because of the above-mentioned reasons, it seems reasonable to explore both mechanisms.

The nonplanar and the planar mechanisms were treated with the 2D-GR and 3D-GR models, respectively. The values of the H-vibrational frequencies were taken from the AM1 force-field output. The effective H-frequencies, needed in 2D-GR, were calculated according to eq 2. The effective frequency and the effective reduced mass of the soft mode were evaluated with eq 3.2 also on the basis of the AM1 force-field output. The values obtained in this way, namely, Ω_{eff} = 58 cm^{-1} and $\mu_{\text{eff}} = 9.8m_{\text{H}}$ for the T_1 enol and Ω_{eff} = 87 cm^{-1} and $\mu_{\text{eff}} = 6.3m_{\text{H}}$ for the T_1 keto form, reproduce the kinetics neither in the planar nor in the nonplanar mechanism. Therefore, these Ω_{eff} and μ_{eff} values were recalculated neglecting the first two lowest-frequency vibrations which are determined with the least certainly in the force-field analysis. This value of μ_{eff} ($5.3m_{\text{H}}$), however, produces poor agreement with the reaction kinetics. As the reduced mass of the effective soft mode is more sensitive to inaccuracies in the force-field calculations, it was chosen to be equal to the reduced mass of the N–O oscillator; thus Ω_{eff} = 195 cm^{-1} and $\mu_{\text{eff}} = 7.5m_{\text{H}}$, where m_{H} is the mass of proton.

The choice of the exothermicity ΔE needs more discussion. As mentioned earlier, the AM1 results do not predict significant distinction between HBO and MHBO as far as the geometries and the keto–enol energy gap ΔE are concerned. To investigate further the method's accuracy and reliability for excited-state analysis it is useful to compare the scheme of S_1 and S_0 levels of HBO extracted from experiment with the AM1 results (Figure 2). The discrepancy between the experimentally observed enol S_1–S_0 gap (Frank–Condon) and the AM1 value calculated as the bottom-to-bottom energy difference is ca. +7 kcal/mol. For comparison, the MNDO/H result for the S_1–S_0 enol gap for HBO is in good agreement with experiment (450 cm^{-1}),[11] while for the S_1 enol–keto gap the agreement between the AM1 and

MNDO/H calculated values and the experimentally observed result is poor (AM1, 5148 cm^{-1}; MNDO/H, 524 cm^{-1};[11] exp, 2100 cm^{-1}). In addition, an error of ca. +6 kcal/mol was reported for a series of 1-(acylamino)anthraquinones where the Frank–Condon S_0–S_1 transitions were obtained using the PM3 approximation and CI calculations with an active space of 20 orbitals.[23] (In our case, the active space consists of 2 orbitals.) For the ground state, the AM1 keto–enol energy gap is ca. 5.5 kcal/mol lower than the experimentally suggested value. Thus, in excited states the AM1 calculations are quite likely to produce a discrepancy of several kcal/mol in the value of ΔE. Also, the method fails to confirm the experimental finding of two different regimes of the triplet ESIPT in HBO and MHBO, reversible and irreversible, respectively. Moreover, if $\Delta E_{K-E} = E_K - E_E < 0$ and is approximately equal to the AM1 result (2.2 kcal/mol), the population of the triplet enol form will no longer be much faster than the triplet keto decay as follows from the experiment.[9,10] Therefore, only two cases are consistent with the spectroscopic data and should be explored for the nonplanar mechanism: (1) $\Delta E_{K-E} > 0$, following the experimental evidence for MHBO with a triplet keto tautomer higher in energy than the enol form, and (2) $\Delta E_{E-K} = 0$, the experimentally suggested quantity for HBO. For the planar mechanism only $\Delta E = 0$ was taken as the AM1 data and the experiment agree relatively well.

With the parameter values chosen, the experimentally observed temperature dependence of the rate of triplet equilibration[9] was compared with

$$\theta_1 = k_{K-E} + k_{E-K} \qquad (6)$$

where $k_{K-E} = k$(keto→enol) and $k_{E-K} = k$(enol→keto) were calculated as rate constants according to eq 5, both for the nonplanar and planar mechanisms. The corresponding curves are depicted in Figure 3a and b, respectively. Unexpectedly, it is the nonplanar mechanism that provides agreement with the kinetics. Though best fit is achieved for isoenergetic states (in qualitative agreement with the experimental evidence for HBO), it is seen that both values of ΔE produce acceptable agreement with the kinetics, taking into account the simplifications of the employed method. This is in accord with the experimentally observed very close resemblance of the kinetic curves for the two compounds, as reported in section II. To continue with our methodological analysis, we have also performed the same calculations for a gap of the opposite sign: $\Delta E_{K-E} = -9.9$ kJ/mol, according to the AM1 findings; the results are also reported in Figure 3a. Comparing the three curves one can conclude that only the experimentally suggested keto–enol arrangements result in agreeable temperature behavior of the observed rate θ_1; the agreement for the AM1 value of ΔE_{K-E} is worse for both isotopes.

Our present model cannot explain why the rate of such a nonplanar transfer is viscosity independent. For this purpose a more detailed picture of such a complicated ESIPT reaction is needed where the skeleton reorganization and the pure H-transfer will be treated more thoroughly, perhaps in a version where the promoting mode (an out-of-plane skeletal bending) is not merely a harmonic oscillator but one subject to relaxation (damped oscillator). Such a treatment, however, is beyond the scope of our approach.

The discussion continues with the analysis of the singlet PT. Generally, the ultrafast singlet ESIPT in the intramolecularly H-bonded species is envisioned either as a barrierless transition in a one-well PES or as tunneling through a low barrier.[1,2] Although the applicability of the GR approach is problematic in the latter case, a semiquantitative comparative GR study of the ground-state and the excited-state PT in this system still can qualitatively assess the relative importance of the geometric, spectroscopic, and electronic factors promoting H-transfer in the excited state as presented below.

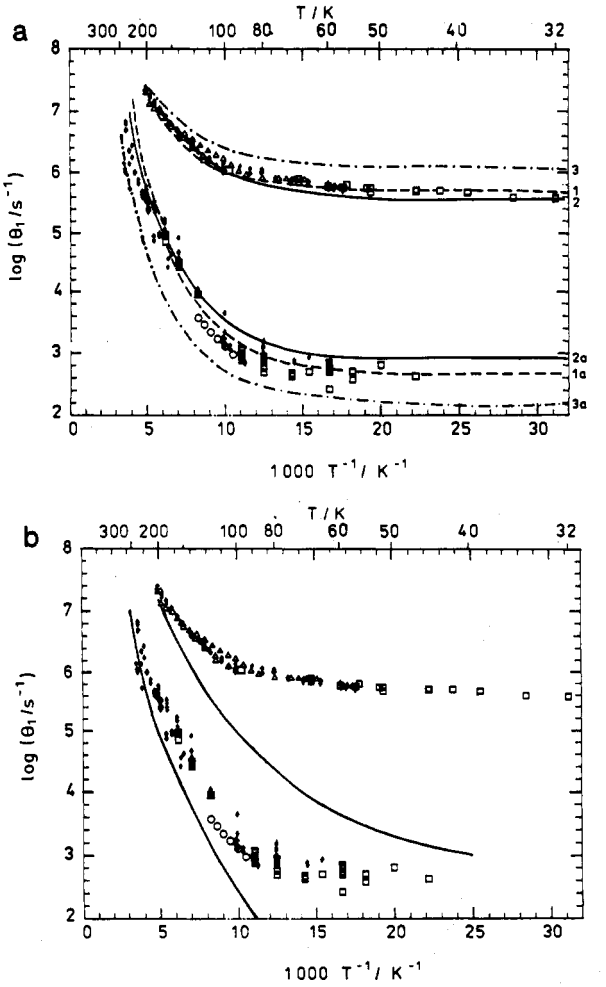

Figure 3. (a) The "nonplanar" triplet ESIPT mechanism in HBO. Curves 1 and 2 represent the GR calculations of θ_1 from eq 6 with exothermicities $\Delta E_{K-E} = 0$ and $\Delta E_{K-E} = 9.9$ kJ/mol, respectively, 1a and 2a being the respective D-curves. Curves 3 and 3a follow the AM1 results of triplet keto–enol arrangement with $\Delta E_{K-E} = -9.9$. Other parameter values: $\omega_{eff}^{NH/D} = 1483/1127$ cm^{-1}, $\omega_{eff}^{OH/D} = 3083/2180$ cm^{-1}, $x^{H/D} = -80/-57$ cm^{-1}; $\Omega_{eff} = 195$ cm^{-1}; $\mu_{eff} = 7.5m_H$; $l = 1.64$ Å; $J_1 = 0.48$ eV, $J_2 = 0.57$ eV, and $J_3 = 0.15$ eV (J is scaled so as to reproduce the experimental value of k_A at 200K). The experimental points represent $\log \theta_1^H$ (upper plot) and $\log \theta_1^D$ (lower plot) measured in three different solvents: 3MP (△), 3MP–IP (◆), IB–CP–MCP (□), plus some phosphorescence data (○), according to ref 9. (b) The "planar" triplet ESIPT mechanism in HBO. A three-dimensional GR mode was employed with H-stretching and bending modes taken explicitly from the AM1 results. The parameters are $\omega_{eff}^{NH} = 3386/1062$ cm^{-1}, $\omega_{eff}^{OH} = 3422/1407$ cm^{-1}, $x^{H/D} = -80/-57$ cm^{-1}; $\Omega_{eff} = 195$ cm^{-1}; $\mu_{eff} = 7.47m_H$; N–O equilibrium distance $R = 2.89$ Å (arithmetic mean of the values for the enol and keto form); $J = 0.69$ eV.

The singlet ESIPT seems to proceed through a barrier, because AM1 located a minimum for the less stable enol structure. The comparative study of the S_0 and S_1 PT (Table II) with the 3D-GR model shows that the differences in geometry, H-frequencies, and exothermicity ΔE can account for a significant, but not dramatic, increase in the rate constant's value in S_1. This is reasonable, as the geometries and the H-frequencies in S_0 and S_1 do not differ dramatically (Table I). According to the AM1 results, the tendency for shortening of the tunneling distance and for increase of ΔE, rather than the changes in the H-frequencies, are responsible for a higher excited-state k_H. The experimental ΔE values also predict an enhancement, though smaller, of the PT rate constant. The above-mentioned parameters, however, are insufficient to explain the high singlet ESIPT rate. Large electronic coupling J is needed to account for it (e.g. $J = 1.06$ eV for the AM1 value of ΔE), as is seen from the results of Table II. This most probably suggests that a low barrier rather than

TABLE II: Rates of Proton Transfer in S_0 and S_1 States of HBO within the 3D-GR Approach[a]

ΔE, kJ/mol	T, K	a_{GR}^H, eV^{-2} s^{-1}
	S_0	
37.9 (AM1)	25	1.6×10^3
	200	2.2×10^6
60.8	25	1.5×10^4
	200	3.9×10^6
	S_1	
63.8 (AM1)	25	5.8×10^6
	200	1.8×10^8
26.0	25	3.7×10^5
	200	2.7×10^7

[a] a_{GR}^H is the rate of H-transfer scaled for $J = 1$ eV. The high-frequency values are listed in Table I; anharmonicity $x_{NH} = x_{OH} = -80$ cm^{-1}; the low-frequency parameters are $\Omega_{eff} = 195$ cm^{-1} and $\mu_{eff} = 7.47 m_H$, m_H is the mass of a proton.

TABLE III: Comparison between the Rates of Singlet and Triplet ESIPT in HBO within 2D-GR[a]

T, K	a_{GR}^H, eV^{-2} s^{-1}
T_1	
25	6.0×10^2
200	4.6×10^4
S_1	
25	1.7×10^3
200	2.2×10^5

[a] a_{GR}^H is as in Table II. The parameters for T_1 are listed in Figure 3a; those for S_1 are $\omega_{eff}^{OH} = 3308$ cm^{-1}, $\omega_{eff}^{NH} = 3171$ cm^{-1}, $\Delta E = 63.8$ kJ/mol, $l = 1.34$ Å; the soft mode parameters are the same as those for T_1.

a deep tunneling mechanism is applicable to the singlet ESIPT. The larger electronic coupling in S_1 than in T_1 is also responsible for the big difference between the singlet and triplet ESIPT rates (Table III). The primary role of the electronic factors in the ESIPT kinetics was also suggested in ref 24 where the singlet ESIPT in three structurally similar H-bonded dimers, 7-azaindole dimer ($k_H > 10^{12}$ s^{-1}), 1-azacarbazole dimer and 7-azaindole-1-azacarbazole heterodimer ($k_H < 10^{12}$ s^{-1}), was studied. The most probable reason for the differences between the ESIPT rates in those species are the differences in the electronic structure, i.e., J and possibly ΔE, as their vibrational frequencies are relatively similar. This example shows that the investigation of structurally similar compounds can be particularly valuable for clarifying some of the factors governing ESIPT. In the present case, a comparative study may be useful of the HBO and its thio analog 2-(2'-hydroxyphenyl)benzothiazole in which the singlet transfer is suggested to be barrierless and no triplet PT was reported.

V. Conclusion

We present a combined Golden Rule–AM1 analysis of the triplet and singlet tunneling dynamics of PT in HBO and MHBO. These compounds express typical non-Arrhenius and very similar temperature behavior of the rate of triplet keto–enol equilibration $\theta_1 = k_{K-E} + k_{E-K}$. A version of the GR approach is applied in which all modes of the transfer atom (stretching, bending, and twisting) are taken into account together with an effective intramolecular promoting mode; the solvent modes are considered responsible for the high density of final states. The input data for the dynamic calculations is the standard output of the AM1 (structural and force-field results) for both tautomers; the electronic coupling J is an adjustable parameter. As in the kinetic experiment, the calculated rate θ_1 is only slightly sensitive to the two experimentally suggested arrangements of the enol and keto triplet states, namely, $\Delta E_{K-E} = 9.9$ kJ/mol (MHBO) and $\Delta E = 0$ (HBO), since both cases result in almost the same kinetic curves (Figure 3a). The same calculations performed for $\Delta E_{K-E} = -9.9$ kJ/mol, (the AM1 result) are in worse agreement with experiment. The study of the singlet ESIPT in these compounds suggests that the primary reason for the rapidity of the process, as well as for the distinctions between the triplet and singlet transfer, is in electronic factors, mainly the electronic coupling.

References and Notes

(1) Barbara, P. F.; Walsh, P. K.; Brus, L. E. *J. Phys. Chem.* **1989**, *93*, 29.
(2) Gillispie, G. D.; Balakrishnan, N.; Vangsness, M. *Chem. Phys.* **1989**, *136*, 249, 259.
(3) Frey, W.; Laermer, F.; Elsaesser, T. *J. Phys. Chem.* **1991**, *95*, 10391.
(4) Al-Soufi, W.; Eychmüller, A.; Grellmann, K. H. *J. Phys. Chem.* **1991**, *95*, 2022.
(5) Mordzinski, A.; Grellmann, K. H. *J. Phys. Chem.* **1986**, *90*, 5503.
(6) Rodriguez Prieto, M. F.; Nickel, B.; Grellmann, K. H.; Mordzinski, A. *Chem. Phys. Lett.* **1988**, *146*, 387. Nickel, B.; Rodriguez Prieto, M. F. *Chem. Phys. Lett.* **1988**, *146*, 393.
(7) Grellmann, K. H.; Mordzinski, A.; Heinrich, A. *Chem. Phys.* **1989**, *136*, 201.
(8) Nagaoka, S.; Itoh, A.; Mikai, K.; Hoshimoto, E.; Hirota, N. *Chem. Phys. Lett.* **1992**, *192*, 532.
(9) Al-Soufi, W.; Grellmann, K. H.; Nickel, B. *J. Phys. Chem.* **1991**, *95*, 10503.
(10) Eisenberger, H.; Nickel, B.; Ruth, A. A.; Al-Soufi, W.; Grellmann, K. H.; Novo, M. *J. Phys. Chem.* **1991**, *95*, 10509.
(11) Arthen-England, Th.; Bultmann, T.; Ernsting, N. P.; Rodriguez, M. A.; Thiel, W. *Chem. Phys.* **1992**, *163*, 43.
(12) Siebrand, W.; Wildman, T. A.; Zgierski, M. Z. *J. Am. Chem. Soc.* **1984**, *106*, 4083, 4089.
(13) Smedarchina, Z.; Siebrand, W.; Wildman, T. A. *Soviet Chem. Phys.* **1989**, *8*, 253.
(14) Smedarchina, Z.; Siebrand, W.; Wildman, T. A. *Chem. Phys. Lett.* **1988**, *143*, 395.
(15) Smedarchina, Z.; Siebrand, W.; Zerbetto, F. *Chem. Phys.* **1989**, *136*, 285.
(16) Goldanskii, V. I.; Trakhtenberg, L. I.; Flerov, V. N. *Tunneling Phenomena in Chemical Physics*; Gordon and Breach: New York, 1988.
(17) Smedarchina, Z. *Chem. Phys.* **1991**, *150*, 47.
(18) (a) Lavtchieva, L.; Smedarchina, Z. *Chem. Phys.* **1992**, *160*, 211. (b) Lavtchieva, L.; Smedarchina, Z. *Chem. Phys. Lett.* **1991**, *184*, 545. (c) *Chem. Phys. Lett.* **1991**, *187*, 506. (d) Chandranupong, L.; Wildman, T. A. *J. Chem. Phys.* **1991**, *87*, 130. (e) Flomenblit, V. Sh.; Miheikhin, I. D.; Trakhtenberg, L. I. *Dokl. Akad. Nauk USSR* **1991**, *320*, 922 (in Russian).
(19) Stewart, J. J. P. MOPAC 6.0, *QCPE* No. 455.
(20) Dewar, M. J. S.; Zoebich, E.; Healy, E.; Stewart, J. J. P. *J. Am. Chem. Soc.* **1985**, *107*, 3902.
(21) Baker, J. *J. Comput. Chem.* **1986**, *7*, 385.
(22) Smedarchina, Z.; Siebrand, W. *Chem. Phys.*, in press.
(23) Smith, T. P.; Zaklika, K. A.; Thakur, K.; Walker, G.; Tominaga, K.; Barbara, P. F. *J. Phys. Chem.* **1991**, *95*, 10465.
(24) Fuke, K.; Kaya, K. *J. Phys. Chem.* **1989**, *93*, 614.